SELF-CONSISTENT SIMULATION OF A BUNCHED ELECTRON BEAM INCLUDING RADIATION, SPACE-CHARGE AND BOUNDARY CONDITIONS

D. R. Gillingham, T. M. Antonsen, Jr., IREAP, University of Maryland, College Park, MD, U.S.A.

Abstract

High-average power Free Electron Laser (FEL) designs will require high-brightness beams. These beams may suffer beam quality degradation during transport through bending sections. Potential mechanisms include microbunching instability and coherent synchrotron radiation. The effects are not well-understood in the transient state, in the presence of conducting boundaries or when these effects operate together and in conjuction with the beam dynamics. A simulation method applicable under the conditions of a MW-class average power FEL driver has been developed that accounts for radiation, space-charge and boundary conditions in a self-consistent manner. This simulation may be useful in evaluating designs concepts under consideration including chicane bunch compression and energy recovery..

INTRODUCTION

An electron bunch traveling along a circular trajectory can emit radiation coherently in as much as the wavelengths of interest are longer than the bunch length. This is called coherent synchrotron radiation (CSR). As the bunch travels along the arc, the CSR will move forward relative to the bunch because of the shorter path length taken by the radiation along the cord of the arc compared to the bunch. For high-brightness electron beam applications, this effect may adversely affect the transverse emittance by energy modulation that breaks the symmetry of an otherwise achromatic or isochronous bending system.

This paper presents a simulation method that can used to estimate possible beam quality degradation by CSR. It is based on a wave equation derived from Maxwell's equations as a perturbation valid when the width of the waveguide, *a*, is small compared to the radius of curvature, *R*, in a bend. This method is otherwise applicable to transient situations with waveguide boundary conditions, and is fully three-dimensional. It automatically includes space-charge. This paraxial wave equation can be combined with a particle-in-cell simulation that provides a means to evaluate beam quality degradation. As an example, emittance growth in a four-dipole chicane is demonstrated.

PARAXIAL WAVE EQUATION

We can numerically solve for the radiation by taking a perturbation of Maxwell's equation for small *x*/*R*, where *x* is the local displacement perpendicular to the main motion in the plane of curvature, using the usual accelerator curvilinear coordinate system. Then, we make a Fourier transform our variables in the longitudinal coordinate, co-moving along the reference trajectory

$$f(z,\mathbf{x}_\perp,s)=\frac{1}{2\pi}\int_{-\infty}^{+\infty}F(k,\mathbf{x}_\perp,s)e^{-ik(s-z)}dk\,. \qquad (1)$$

The resulting wave equation for the evolution of the fields, originally presented in [1], modified to include finite γ is

$$2ik\frac{\partial}{\partial s}\mathbf{E}_\perp(k)=-\left[\nabla_\perp^2+k^2\left(\frac{2x}{R}-\frac{1}{\gamma^2}\right)\right]\mathbf{E}_\perp(k)+4\pi\nabla_\perp\rho(k) \qquad (2)$$

where:

$\mathbf{E}_\perp(k)$ = Fourier transform of perpendicular electric field vector;
γ = reference trajectory relativistic factor;
ρ = charge density; and
$\nabla_\perp$ = indicates gradient operator in x-y plane.

The longitudinal field can be found from the perpendicular components using Poisson's equation:

$$\nabla\cdot\mathbf{E}(\mathbf{x})=-4\pi\rho(\mathbf{x})\,. \qquad (3)$$

In Fourier-space, this can be solved under the same perturbation:

$$E_z(k)=\frac{i}{k}\left(\frac{\partial E_x}{\partial x}+\frac{\partial E_y}{\partial y}-4\pi\rho\right). \qquad (4)$$

Also, under the same paraxial assumption, the electron current in directions other than along the axis can be neglected, and therefore will only generate a magnetic field along the principle axis of motion. The Fourier-space solution of the magnetic field is:

$$B_z(k)=\frac{i}{k}\left(\frac{\partial E_x}{\partial y}-\frac{\partial E_y}{\partial x}\right). \qquad (5)$$

We are now in a position to compute all of the Lorentz forces generated by the three electric and one magnetic field components which are:

$$F_x(k)=e\left\{\frac{i}{2k}\left(\frac{\partial B_z}{\partial y}-\frac{\partial E_s}{\partial x}\right)+\frac{E_x}{2\gamma^2}\right\}, \qquad (6)$$

$$F_y(k) = e\left\{\frac{-i}{2k}\left(\frac{\partial B_z}{\partial x} - \frac{\partial E_s}{\partial y}\right) + \frac{E_y}{2\gamma^2}\right\}, \quad (7)$$

$$F_z(k) = eE_z\,. \quad (8)$$

That these forces include space-charge can best be shown using an eigenfunction expansion which will be explained in the simulation methods section.

BEAM DYNAMICS

For the purposes of simulation, the electron beam dynamics resulting from the Lorentz forces (6)-(8), must be combined with the usual relativistic curvilinear dynamics to account for chromatic and dispersive effects. Specifically here, we will only describe dispersion to first order in energy deviation, although this could be improved in the future. Additionally, other terms have been neglected under the assumption relatively small changes in energy. The approximate equations of motion for individual electrons are:

$$x'' \equiv \frac{d^2x}{ds^2} = \frac{\Delta\gamma}{\gamma R} - \frac{x}{R^2} + \frac{F_x}{\gamma m_e c^2} \quad (9)$$

$$y'' = \frac{F_y}{\gamma m_e c^2} \quad (10)$$

$$z' = -\frac{x}{R}, \text{ and} \quad (11)$$

$$\Delta\gamma' = \frac{F_z}{m_e c^2}\,. \quad (12)$$

SIMULATION METHODS

In integrating (2), we use a pseudo-spectral method instead of finite-differencing, which forces the transverse boundary conditions. Specifically, we split the integration step into two steps corresponding to the terms involving x and $\nabla_\perp$ respectively. The second operator is integrated by first transforming into in only sine or cosine terms, depending on the applicable boundary conditions, so that the transverse Laplacian transforms from $\nabla_\perp^2 \rightarrow -k_\perp^2$. Therefore, equation (2) becomes the following two equations that are integrate each step:

$$\frac{d\mathbf{E}_\perp(\mathbf{x}_\perp)}{ds} = \frac{ikx}{R}\mathbf{E}_\perp \quad (13)$$

$$\frac{d\tilde{\mathbf{E}}_\perp(\mathbf{k}_\perp)}{ds} = -\frac{i}{2k}\left(k_\perp^2\tilde{\mathbf{E}}_\perp + 4\pi\mathbf{k}_\perp\tilde{\rho}\right). \quad (14)$$

where the ~ superscript indicates the coefficient of an expansion in products of cosine and sine terms appropriate for the boundary conditions. To be specific, the expansions are:

$$E_x = \sum_{n=0}^{\infty}\sum_{m=0}^{\infty}\tilde{E}_x^{nm}\cos[k_x(x-a/2]\sin(k_y(y-b/2)] \quad (15)$$

$$E_y = \sum_{n=0}^{\infty}\sum_{m=0}^{\infty}\tilde{E}_y^{nm}\sin[k_n(x-a/2]\cos(k_m(y-b/2)] \quad (16)$$

where $k_x = n\pi/a$ and $k_y = m\pi/b$. In practice, these are replaced by their finite, or discrete forms. By looking at the case of no curvature ($R\rightarrow\infty$), and steady state, we easily obtain the space-charge fields:

$$\tilde{\mathbf{E}}_\perp^{SS} = -\frac{4\pi\mathbf{k}_\perp\tilde{\rho}}{(k_\perp^2 - k^2/\gamma^2)}, \quad (17)$$

where $\mathbf{k}_\perp = k_x\mathbf{e}_x + k_y\mathbf{e}_y$.

Putting (17) into (4)-(6) and expanding to order $1/\gamma^2$,

$$\tilde{F}_x^{ss} \approx -\frac{4\pi k_x\tilde{\rho}}{k_\perp^2\gamma^2}, \quad (18)$$

$$\tilde{F}_y^{ss} \approx -\frac{4\pi k_y\tilde{\rho}}{k_\perp^2\gamma^2}, \quad (19)$$

$$\tilde{F}_z^{ss} \approx \frac{4\pi ik\tilde{\rho}}{k_\perp^2\gamma^2}\,. \quad (20)$$

Note that each component has the usual $1/\gamma^2$ dependence as expected and represent the space charge forces for the beam in a drift section.

To complete the simulation, the charge density in (4) and (14) can be computed from a cloud-in-cell interpolation of an ensemble of macro-particles, and then integrated according to (9)-(12). To keep the results accurate to second-order in time, a slightly complicated leapfrog sequence is implemented in the following order:

1. x' and y' (half-step)
2. Fields (half-step)
3. z (half-step)
4. γ
5. x and y
6. z (half-step)
7. Fields (half-step)
8. x' and y' (half-step)

RESULTS

To test the method, a benchmark four-dipole chicane design, shown in figure 1 was integrated using the parameters listed in table 1 and 2. No pulse compression (i.e. no energy chirp applied to pulse) was used at this time, because matters related to stability of this scheme have not been solved for a rapidly evolving beam distribution.

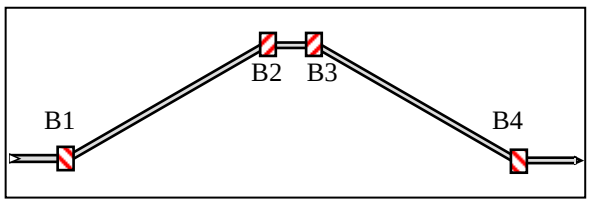

Figure 1. Four-dipole chicane. The rectangles, B1-B4 represent hard-edge magnets. The grey sections indicate the rectangular waveguide.

As an example of the complexity of the difficulty in calculating CSR in a waveguide from theory, the longitudinal electric field, taken at the mid-plane (y=0) of the waveguide as a function of x and z is shown (Fig. 2). In this coordinate system, recall that negative z is ahead of the reference point and x is positive away from the initial curvature. The field is normalized to the steady-state longitudinal electric field for a Gaussian pulse [2]:

$$W_0 = \sqrt{\frac{2}{\pi}} \frac{Ne^2}{(3R^2\sigma^4)^{1/3}} \qquad (15)$$

where:
N = number of electrons in bunch,
e= charge of electron,
σ= pulse length (rms) of Gaussian bunch,

Table 1. Chicane parameters.

Bend magnet length (projected)	0.5 m
Drift length (projected)	5.0 m
Bend radius	10.35 m
Bending angle	2.77^o
Vertical gap	5 mm

Table 2. Electron beam parameters.

Nominal energy	500 MeV
Bunch charge	1.0 nC
Incoherent energy spread	10 keV
Bunch length, rms	20 mm
Normalized emittance	1 mm-mrad
Initial betatron function	10 m
Initial alpha function	0.0

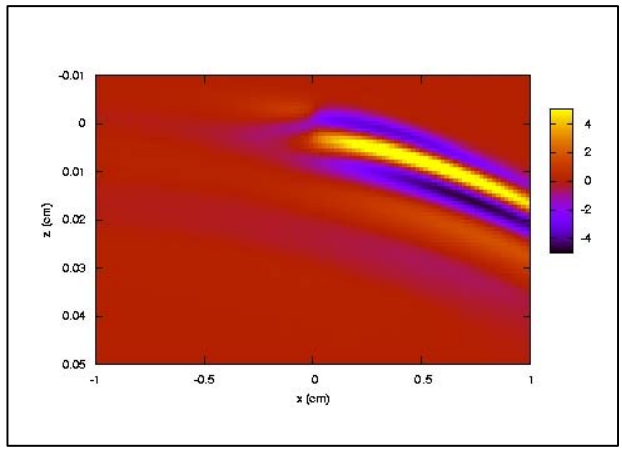

Figure 2. Longitudinal electrical field,, normalized to W_0 (15), at mid-plane (y=0) of rectangular waveguide (5 cm wide by 0.5 cm tall) as a function of x and z, at the exit of the first bending magnet.

The dominant effect of coherent synchrotron radiation is to modulate the energy of the bunch in the bending magnet sections. This effect is shown in figure 3 Then, dispersion leads to transverse emittance growth primarily by a correlated effect on x' (vs. z), which when projected onto x-x' phase space for the entire bunch increases the area occupied by the coordinates of the electrons as shown in figure 4.

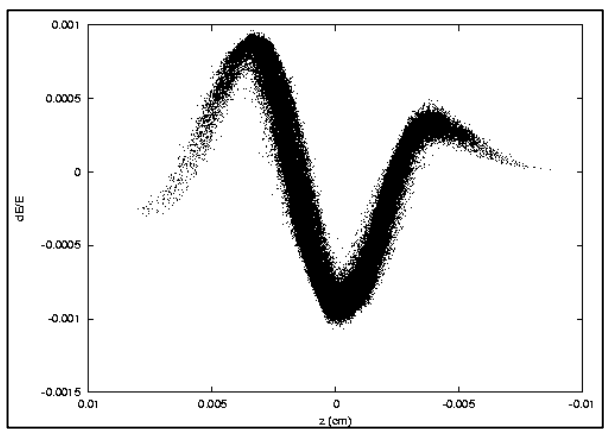

Figure 3. Energy deviation as a function of position within the bunch, taken at the midpoint (drift space between second and third bending magnets), showing the effect of coherent synchrotron radiation

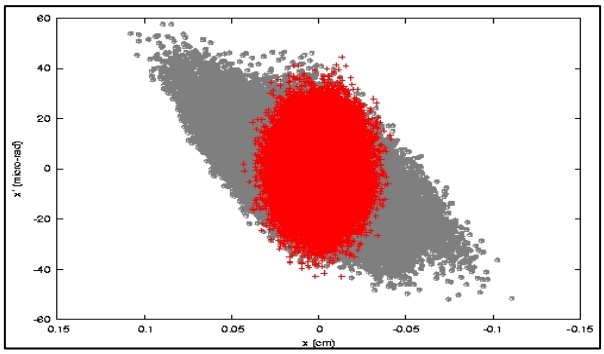

Figure 3. Phase space plot at end of chicane with no chirp. The projected normalized x-emittance growth is approximately 2.6 mm-mrad.

CONCLUSIONS

The model shows several promising features over previous methods of calculating CSR. Specifically, it takes the boundary conditions into account explicitly, is fully three-dimensional, includes space charge, and is valid in transient conditions. Furthermore, because it does not neglect the formation time, it may be suitable for the study of potential instabilities.

This model does however have limitations as well, the most notable of which is the assumption of periodicity implicit in the use of the longitudinal Fourier transform. Finally, it lacks a realistic model for attenuation due to finite resistivity of the walls. Research continues in these areas as well as improvement in the theory of CSR.

ACKNOWLEDGEMENTS

This work was carried out with the support the Office of Naval Research and the Joint Technology Office.

REFERENCES

[1] T. Agoh, K. Yokoya, *"Calculation of coherent radiation using mesh"*, PRST-AB **7**, 2004, p. 054403.

[2] J. B. Murphy, S. Krinsky, and R. L. Gluckstern, *"Longitudinal wakefield for an electron moving on a circular orbit"*, Part. Accel. **57**, 1997, p. 9.